

**GSA Data Repository 2011023
Supplemental Information**

Low marine sulfate concentrations and the isolation of the European Epicontinental Sea during the Early Jurassic

Newton et al.

SAMPLING, GEOLOGICAL SETTING & PALAEOGEOGRAPHY

Samples were collected on the north Yorkshire coast in the UK from Runswick Bay, Kettleness point and at Ravenscar. Belemnite samples were collected from both these locations, collecting the best stratigraphic coverage possible from each different formation. A collection of 56 samples were analysed. The belemnites had their outer surface and phragmacone region removed by grinding or diamond saw (see below), and were then crushed with a mechanical agate pestle and mortar and sieved to 150 microns.

Kioto Group limestone samples from Tibet were collected from a recent road cutting along the Peru–Pang La road near Yungia village (see Wignall et al., 2006 for more detail), avoiding veins and weathered surfaces. Lithologies ranged between oolitic or calcarenitic packstones and grainstones, bioclastic wackestones and thinly bedded limestones. 29 samples were analysed. In as far as it was possible, all limestone samples were trimmed of any veins and weathering surfaces (both of which might introduce secondary sulphate contamination) using a diamond saw, and then pulverised using a TEMA agate mill.

The palaeogeography of the European epeiric sea is relatively well known, and the Yorkshire section is separated from the open Tethyan or Boreal ocean by at least 1000 miles of shallow sea with a complicated palaeogeography. The Tibetan section could still be classed as epeiric in the sense that these sediments were deposited on the edge of a continental landmass but are likely to have been much closer to the open ocean and with little or no geographic barriers. Jadoul et al, (1998) describe the Tibetan palaeogeographic setting as occurring on a passive margin. On this margin similar successions of Mesozoic sediments occur throughout the Himalayas, and the Kioto limestones which we sampled have correlatable equivalents ‘from the whole of the Tethys Himalaya’, suggesting a relatively narrow linear strip of deposition at the edge of the continent, entirely different from the extensive shallow sea that occupied Europe.. Deeper water sediments described as being deposited in a shelf to distal ramp setting are present to the north and west within 20 to 100km, further reinforcing the evidence for short distances to the open ocean. Moreover, sediment deposition in the Tethyan Himalaya was clearly starved of clastic inputs during the Toarcian-Aalenian interval as it is dominated by carbonate sediments (carbonate ranges from 74 to 99 wt%, mean = 92 wt% in our samples (Table DR1), although there are more frequent thin 2-5cm shale inter-beds in the upper K2 part of the section, which we did not sample. This is relevant for the CAS sulfate isotope records because the main driver of regional isotopic differentiation and the development of global ocean-epeiric sea isotopic gradients is likely to be the regional pyrite burial flux. High pyrite fluxes require regional sources of reactive iron and organic matter. The reactive iron flux is proportional to clastic input and is therefore very much reduced in the Tethyan Himalaya sediments during the time in question. Organic matter contents of the sediments are also very low, between 0.1 and 0.18 wt%, mean = 0.07 wt% (Table DR1), further indicating that large regional pyrite fluxes were very unlikely in this palaeogeographic setting.

Thus, it follows that the Tibetan section is both more likely to have experienced rapid mixing with the open ocean waters, and less likely to have been able to produce the large regional pyrite fluxes required to develop global ocean-epeiric sea sulfate isotope gradients. Hence the Tibetan section records the sulfate isotope composition of the global ocean without significant modification. The water masses from the Cleveland sub-basin of the European Epeiric Sea in contrast, would mix with open marine waters on much longer timescales because of the sheer distance and complexity of the pathway to the open ocean. The sediments beneath the water masses from this and other nearby sub-basins were dominated by clastic sedimentation and had large inventories of organic carbon, providing ideal conditions for enhanced regional fluxes of pyrite sulfur. Therefore the dissolved sulfate isotope composition of the much of the European Epeiric Sea is distinctly prone to modification with respect to the global ocean signal.

METHODS

Belemnites; SEM and Cathodoluminescence

Thirteen samples were examined by SEM; 10 of them were examined both in polished blocks and in fractured surfaces, the other 3 only as fractured surfaces. These samples were selected to determine the levels of other sulfur bearing phases within the belemnite calcite and to check the degree of alteration and secondary calcite growth. Samples were selected from a representative variety of lithologies to determine any systematic patterns of mineralization or alteration were present.

One sample was from Cleveland Ironstone Formation (CIF, sample id 43), four samples (sample id's 21, 28 and 31 and an additional sample not analysed for CAS, id 37 at 12.3 m,) were from the Grey Shale Member (GSM), another four (8, 9, 14 and 13) from the Jet Rock (JR), samples 19 and RS-34 were from the Bituminous Shales (BS), RS-13 from Peak Mudstone Member and last RS-2, from the Yellow Sandstone Member. The 9 samples from the CIF, GSM and the JR were also studied under cathodoluminescence (CL).

The samples were set in 30mm resin blocks and carbon coated. The SEM used was a CamScan Series 4, and was operated at 20kV in backscattered mode. EDS spectra were acquired using an Oxford MicroAnalysis Division Link 10/255 EDS.

For cathodoluminescence the samples were examined using a Technosyn Cold Cathode Luminescence Model 8200 MK II. The pictures were taken with an Olympus BH-2 camera, on 800 ASA film.

SEM and Cathodoluminescence results

Examination of the belemnites revealed similar levels of alteration and additional sulfur bearing minerals from all lithologies, suggesting that lithologically driven differences in diagenetic environment could not have produced systematic changes such as those observed in the dataset. Barite, pyrite and more rarely, sphalerite, were all observed to occur within the belemnite calcite and often in higher concentrations near the outer surface, which was removed by grinding before crushing for this reason. Luminous calcite, presumed to represent secondary calcite growth, was observed in all samples with a similar extent of alteration in all lithologies. Alteration was concentrated along the apical line, in particular growth rings, and following micro-fractures (e.g. Figure DR1 and Figure DR2). Luminous material and other sulfur bearing phases were also especially concentrated in the phragmacone region so this was also removed.

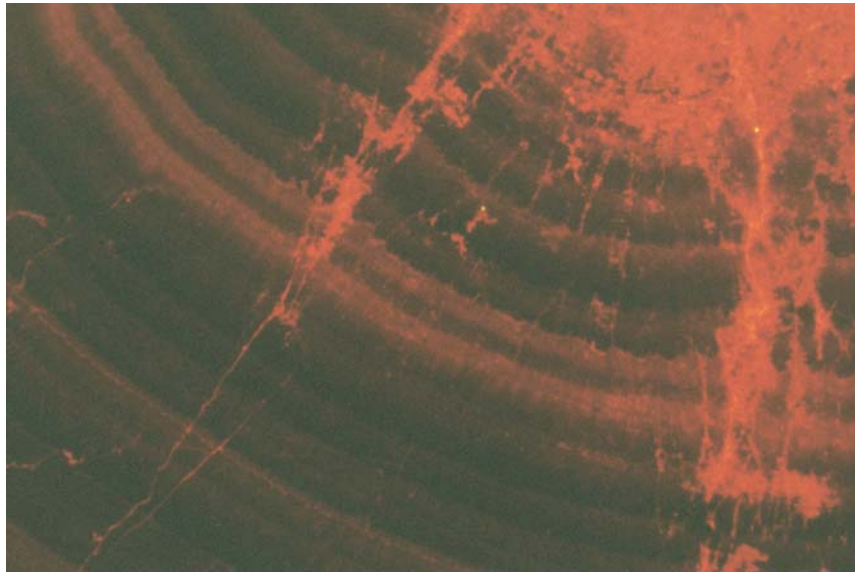


Figure DR1. Luminous calcite concentrated along the apical line (top right) and extending out along micro-fractures

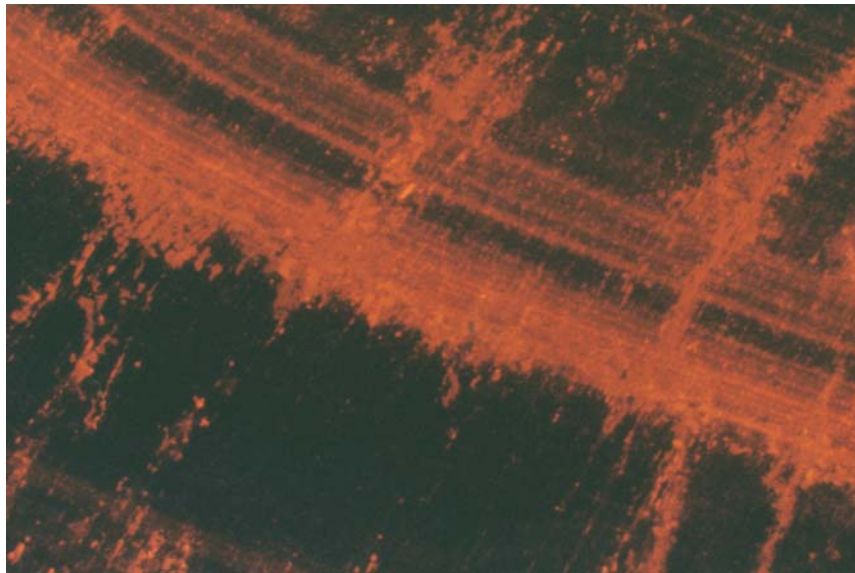


Figure DR2. Luminous calcite concentrated along growth lines.

CAS EXTRACTION

The procedure followed is that of Burdett et al (Utrilla et al., 1992) with minor modifications. The powdered samples were left in an excess of sodium hypochlorite (NaOCl) 5% (v/v) for at least 24 hours, to remove sulfur contained in organic matter, and sulphate or sulphide minerals. Bleached powders were subsequently vacuum filtered onto Whatman GCA glass microfibre filters.

The bleached and rinsed powder was reacted with 50% (w/v) HCl in an anaerobic environment (a Coy anaerobic chamber for the belemnite samples, an argon glove bag for the bulk carbonate samples) in order to release the CAS from the calcite lattice and avoid oxidation of any surviving sulphide minerals. The 50% (w/v) HCl was added until there was no more reaction. The solution was filtered through a Whatman 40 filter paper. When the samples were out of the chamber, they were immediately vacuum filtered through a 0.45 µm filter paper. The pH was adjusted to >9.5 with concentrated ammonia solution and the samples left stirring overnight or longer. The precipitated metals and the leachate were separated using a Whatman 40 filterpaper. Finally, BaSO₄ was precipitated from the HCl leachate by adjusting the pH to between 2.5 and 3 with HCl and ammonia solution, and adding 10% w/v BaCl₂ solution in excess at 70°C. The weight of BaSO₄ precipitate was measured to determine the CAS yield. This gravimetric was corrected for purity using the wt% sulfur derived during isotopic analysis. Subsamples of the BaSO₄ precipitate powders were analysed for sulphur and oxygen isotope composition.

ISOTOPE ANALYSES

Sulfate-S isotopic analyses were performed on a Micromass Isoprime continuous flow mass spectrometer coupled to a Eurovector Elemental Analyser. BaSO₄ was weighed out in tin cups and converted to SO₂ by flash combustion at 1020 °C in the presence of oxygen. Excess oxygen is removed by reaction with hot copper at 650 °C and the SO₂ is separated from other impurities using a chromatographic column and a helium carrier gas. ³⁴S/³²S is derived from the integrated mass 66 and 64 signals from the pulse of sample SO₂, compared to those in an independently introduced pulse of reference gas. These ratios are then calibrated using an internal seawater derived barium sulfate standard (SWS-3a, +20.3‰), and CP-1 a chalcopyrite inter-laboratory standard (-4.56‰, value from SURRC at East Kilbride). The values for CP-1 and SWS-3a were checked and calibrated respectively using IAEA-S1 (-0.30‰), IAEA-S3 (-32.06‰) and NBS-127 (+20.3‰) international standards to the Vienna-Canyon Diablo Troilite (V-CDT) scale in per mille notation (‰). The precision obtained for repeat analysis of standard materials is better than ± 0.3‰ (1 standard deviation).

To analyse for the isotopic composition of the oxygen in the sulphate ion the barium sulphate precipitates were mixed with spectroscopic graphite and placed onto platinum foils, degassed and conductively heated under vacuum to about 1100 °C. A quantitative yield of CO₂ was achieved by converting any CO to CO₂ using a high voltage applied across platinum electrodes, whilst water was removed cryogenically. The ¹⁸O/¹⁶O ratios were measured on the CO₂ gas using VG SIRA 10 dual inlet, 90° magnetic sector gas source mass spectrometer and calibrated to the Vienna-Standard Mean Ocean Water (V-SMOW) scale using an internal standard (SWS-3a), previously calibrated to the international standard NBS-127 (9.34‰) and assigned a value of +9.70‰. The precision obtained for repeat analysis of standard materials is generally better than ± 0.5‰ (1 standard deviation)

DATA EVALUATION

Five CAS sulfur isotope data points (sample ids K1-04, K1-10, K1-12, K2-32, and K2-37) in the Tibetan dataset record ³⁴S depleted values, quite distinct from stratigraphically adjacent data (Figure DR3, Table DR1). These samples also record amongst the lowest CAS-oxygen isotope values in the dataset (FigureDR4, Table DR1). These are considered to be an artefact and not to represent original seawater composition for a number of reasons. Several of these are not diagnostic individually but taken together provide a strong case for their exclusion:

- 1) The changes are not part of an long term trend but are interspersed with much more positive $\delta^{34}\text{S}$ values (Figure DR3)
- 2) These values are mostly substantially below the only other estimate for early Jurassic seawater sulfate- ^{18}O and ^{-34}S (11.7 and 19.1‰ respectively, FigureDR4) derived from evaporites (Utrilla et al., 1992).
- 3) Several of these samples also produced relatively large amounts of sulfur during the sodium hypochlorite leach (Table DR1). This suggests that these samples had greater amounts of sulfur in non-CAS form available for contamination.
- 4) These outlying values can be readily explained by sulfide oxidation processes occurring either in the original porewaters or during the extraction process itself. Sulfides either dissolved or solid generally have a very different sulfur isotopic composition compared to the sulfate from which they were formed because of the large fractionation imposed by bacterial sulfate reduction. Measurement of the isotopic composition of sulfur removed by the hypochlorite pre-treatment records values of 1.4 to -16.8‰ $\delta^{34}\text{S}_{\text{VCDT}}$ with a mean of -7.1‰ confirms that the sum of sulfide plus organic sulfur in the Tibetan carbonate sediments conforms to this generalisation. Any addition of this sulfur to the CAS pool will therefore shift its sulfur isotopic composition to more negative values, although the exact size of this shift will depend on the isotopic composition of the contaminating sulfur which is highly variable (see table). Oxidation of this sulfur can also affect the oxygen composition of the sulfate produced particularly during the extraction process because here all the oxygen must derive from the water. Both the lab distilled water and the original porewater will be substantially less ^{18}O rich than that of marine sulfate (0‰ seawater, -approximately -7‰ lab distilled water) anaerobic sulfide oxidation will also shift the sulfate-oxygen isotope composition to more negative values, as seen in the data. Sulfide oxidation is possible during the CAS extraction because very fine grained sulfide minerals can survive the bleaching pre-treatment by inclusion in larger carbonate grains. These can then be oxidised anaerobically by metal species released during the CAS extraction.

The data in question are therefore removed from the database when calculating mean isotope values for comparison with the Yorkshire data.

CAS-S isotope data from Yorkshire displays a clear change in moving average value across the thick black shale known as the Jet Rock, present in the uppermost *tenuicostatum* and lower *falciferum* ammonite zones. Isotopic variability in the groups of data below, and above, the Jet Rock has a very similar variability to that recorded in the Tibetan data. A few datapoints seem to be obvious outliers, but because they do not have an obvious and consistent relationship with their $\delta^{18}\text{O}$ composition and since these represent a much smaller proportion of the whole database they have been retained.

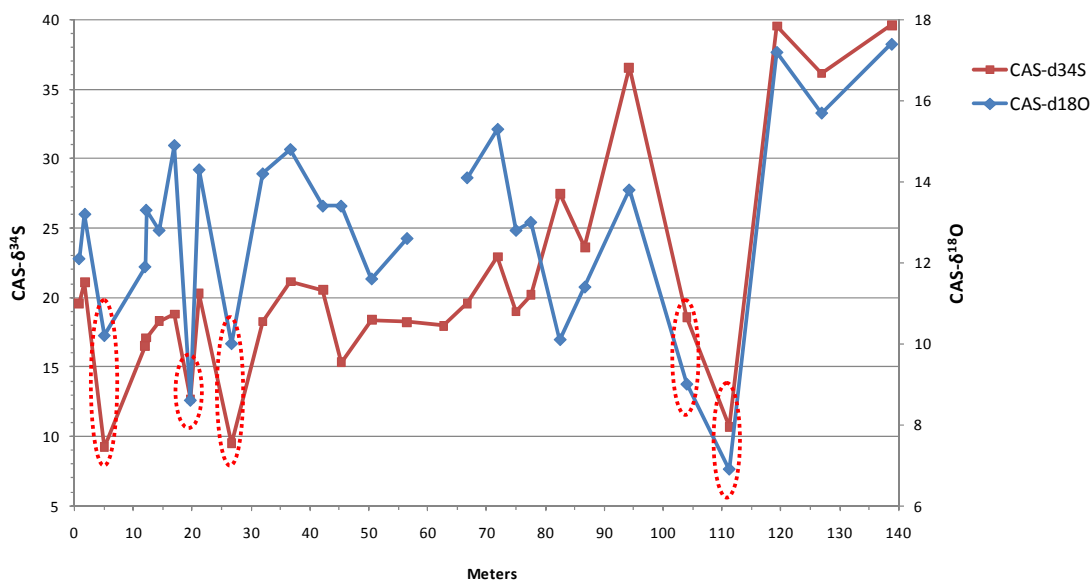


Figure DR3. Tibetan CAS-S and CAS-O isotope data plotted against height. Note the five pairs of values (circled) which have markedly low $\delta^{34}\text{S}$ values compared to stratigraphically adjacent samples. These samples also have low CAS- $\delta^{18}\text{O}$ values.

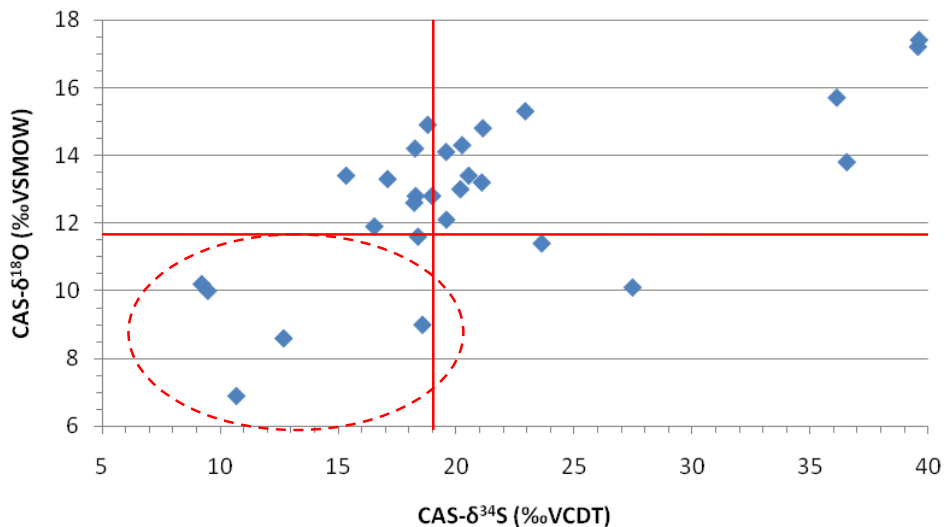


Figure DR4. Tibetan CAS-S vs CAS-O isotope data. Solid red lines are average isotope compositions of Liassic anhydrite (Pálffy et al., 2000). Note the five values (circled) with $\delta^{34}\text{S}$ and $\delta^{18}\text{O}$ less than the evaporite average. These samples have markedly low $\delta^{34}\text{S}$ values compared to stratigraphically adjacent samples.

Table DR1. Tibetan isotope and concentration data (blank = not analysed, red lettering = samples whose CAS-S data are suspected of contamination during extraction)

Sample	Height (m)	CAS-S (ppm)	$\delta^{34}\text{S}_{\text{CAS}}$ (‰ V-CDT)	$\delta^{18}\text{O}_{\text{CAS}}$ (‰ VSMOW)	Hypochlorite-S (ppm)	$\delta^{34}\text{S}_{\text{hypochlorite-S}}$ (‰ VCDT)	TOC (wt%)	$\delta^{13}\text{C}_{\text{Org}}$ (‰ VPDB)	Inorganic carbonate as calcite (wt%)	$\delta^{13}\text{C}_{\text{Carb}}$ (‰ VPDB)
K1-01	0.8	69	19.6	12.1	28	-0.9	0.10	-25.0	89.2	1.2
K1-03	1.8	14	21.1	13.2	52	0.7	0.02		96.1	0.9
K1-04	5.1	34	9.2	10.2	176	-16.8	0.08	-25.2	97.9	1.5
K1-05	7.0						0.01		76.3	1.0
K1-06	12.0	13	16.5	11.9	36	-8.1	0.02	-25.2	87.4	0.0
K1-07	12.2	24	17.1	13.3	35	-4.1	0.05	-26.9	98.0	0.7
K1-08	14.4	32	18.3	12.8	30	-0.4	0.06	-26.6	96.8	0.7
K1-09	17.0	7	18.8	14.9	26	-12.3	0.03	-23.6	88.5	1.4
K1-10	19.7	8	12.7	8.6	22	-7.1	0.03	-25.3	89.7	1.6
K1-11	21.2	28	20.3	14.3	28	-16.1	0.07	-24.5	87.6	1.4
K1-12	26.7	27	9.5	10.0	22	-9.4	0.02	-21.2	97.4	2.1
K1-13	32.0	34	18.3	14.2	21	-3.4	0.03	-21.7	98.1	2.3
K1-14	36.7	18	21.1	14.8	16	-2.2	0.06	-24.3	98.3	2.1
K1-15	42.2	16	20.5	13.4	31	-12.5	0.04	-22.5	97.0	2.0
K1-17	45.3	36	15.3	13.4	26	-2.0	0.02	-24.9	95.3	0.7
K1-19	50.5	30	18.4	11.6	41	-14.3	0.05	-24.8	94.4	1.8
K1-22	56.5	31	18.2	12.6	17	-8.9	0.04	-25.3	98.7	1.6
K1-24	62.7	2	18.0		9	0.7	0.03	-25.9	99.3	0.8
K1-27	66.7	23	19.6	14.1	12	-0.4	0.03	-25.5	98.2	1.4
K1-30	71.9	40	22.9	15.3	14	-5.0	0.07	-25.1	97.4	2.1
K1-33	75.0	22	19.0	12.8	122	-16.6	0.09	-26.3	97.0	1.8
K2-04	77.5	3	20.2	13.0	27		0.07	-24.9	74.1	1.3
K2-11	82.5	25	27.5	10.1	29		0.04	-25.8	82.0	1.8
K2-16	86.7	13	23.6	11.4	120	1.4	0.17	-26.4	88.8	1.9
K2-20	90.0						0.18	-25.8	86.2	1.8
K2-26	94.2	18	36.5	13.8	58		0.09	-23.1	92.5	1.6
K2-29	99.1						0.09	-25.6	91.1	1.9

Sample	Height (m)	CAS-S (ppm)	$\delta^{34}\text{S}_{\text{CAS}}$ (‰ V-CDT)	$\delta^{18}\text{O}_{\text{CAS}}$ (‰ VSMOW)	Hypochlorite-S (ppm)	$\delta^{34}\text{S}_{\text{hypochlorite-S}}$ (‰ VCDT)	TOC (wt%)	$\delta^{13}\text{C}_{\text{Org}}$ (‰ VPDB)	Inorganic carbonate as calcite (wt%)	$\delta^{13}\text{C}_{\text{Carb}}$ (‰ VPDB)
K2-32	104.0	30	18.6	9.0	60	-12.3	0.06	-26.7	94.3	1.2
K2-35	108.3						0.08	-26.3	92.8	1.3
K2-36	109.9						0.10	-25.8	90.5	1.2
K2-37	111.2	67	10.7	6.9	188	-12.6	0.07	-22.7	93.7	1.2
K2-38	111.9						0.10	-25.8	85.5	1.0
K2-39	113.1						0.10	-25.9	92.1	1.5
K2-40	114.3						0.09	-25.4	93.1	1.6
K2-41	115.8						0.11	-26.3	93.7	1.6
K2-43	119.3	55	39.5	17.2	11		0.12	-25.2	90.1	1.7
K2-45	123.9						0.10	-25.6	94.4	1.8
K2-46	126.9	42	36.1	15.7	20		0.09	-23.8	88.9	1.7
K2-47	129.8						0.14	-25.6	90.0	1.6
K2-50	135.9						0.08	-25.0	86.3	1.2
K2-51	138.8	21	39.6	17.4	22		0.09	-23.4	93.7	1.6
K2-52	143.0						0.03	-24.6	98.9	0.9

Table DR2. Yorkshire belemnite CAS isotope data.

Sample Id	Height (m)	CAS $\delta^{34}\text{S}_{\text{VCDT}}$	Ammonite zone	Lithological unit
RS-2	138.1	14.2	<i>levesqui</i>	Yellow Sandstone Member
RS-3	135.9	20.5	<i>levesqui</i>	Yellow Sandstone Member
RS-7	132.6	22.2	<i>levesqui</i>	Yellow Sandstone Member
RS-5	131.5	19.7	<i>levesqui</i>	Grey Sandstone Member
RS-8	124.3	20.5	<i>levesqui</i>	Grey Sandstone Member
RS-10	122.7	22.6	<i>levesqui</i>	Fox Cliff Siltstone Member
RS-11	114.2	21.7	<i>thouarsense</i>	Fox Cliff Siltstone Member
RS-13	109.8	20.9	<i>thouarsense</i>	Peak Mudstone member
RS-14	103.6	21.7	<i>variabilis</i>	Peak Mudstone member
RS-17	101.7	22.6	<i>variabilis</i>	Peak Mudstone member
RS-18	96.9	21.3	<i>variabilis</i>	Cement Shales
RS-21	77.2	23.4	<i>bifrons</i>	Cement Shales
RS-24	71.8	22.1	<i>bifrons</i>	Main Alum Shales
RS-25	69.6	21.4	<i>bifrons</i>	Main Alum Shales
RS-27	66.05	21.8	<i>bifrons</i>	Main Alum Shales
RS-28	61.9	21.1	<i>bifrons</i>	Main Alum Shales
RS-29	55.2	23.3	<i>bifrons</i>	Hard Shales
RS-30	51.1	22.1	<i>falciferum</i>	Bituminous Shales
RS-31	46.6	23.7	<i>falciferum</i>	Bituminous Shales
RS-34	36	21.1	<i>falciferum</i>	Bituminous Shales
RS-33	34.4	24.2	<i>falciferum</i>	Bituminous Shales
RS-35	29	21.4	<i>falciferum</i>	Bituminous Shales
19	25.15	20.5	<i>falciferum</i>	Jet Rock
18	24.9	21.0	<i>falciferum</i>	Jet Rock
15	24.4	19.9	<i>falciferum</i>	Jet Rock
16	23.5	22.5	<i>falciferum</i>	Jet Rock
13	23.2	21.2	<i>falciferum</i>	Jet Rock
14	22.8	20.7	<i>falciferum</i>	Jet Rock
11	22.65	20.7	<i>falciferum</i>	Jet Rock
12	22.45	18.1	<i>falciferum</i>	Jet Rock
17	22.25	21.6	<i>falciferum</i>	Jet Rock
10	22.15	20.0	<i>falciferum</i>	Jet Rock
7	21.75	19.6	<i>falciferum</i>	Jet Rock
9	21	18.7	<i>falciferum</i>	Jet Rock
8	20.6	14.8	<i>falciferum</i>	Jet Rock
48	17.8	16.9	<i>tenuicostatum</i>	Grey Shales Member
31	17.5	15.9	<i>tenuicostatum</i>	Grey Shales Member
32	16.85	16.7	<i>tenuicostatum</i>	Grey Shales Member
33	15.5	16.4	<i>tenuicostatum</i>	Grey Shales Member
28	14.9	16.4	<i>tenuicostatum</i>	Grey Shales Member
29	13.4	18.4	<i>tenuicostatum</i>	Grey Shales Member
38	13.1	16.9	<i>tenuicostatum</i>	Grey Shales Member
30	11.3	16.8	<i>tenuicostatum</i>	Grey Shales Member
36	10.8	17.3	<i>tenuicostatum</i>	Grey Shales Member
21	9.7	17.9	<i>tenuicostatum</i>	Grey Shales Member
22	9.5	16.1	<i>tenuicostatum</i>	Grey Shales Member
23	8.9	13.6	<i>tenuicostatum</i>	Grey Shales Member
25	8.6	16.2	<i>tenuicostatum</i>	Grey Shales Member
41	7.95	16.9	<i>tenuicostatum</i>	Grey Shales Member
46	5.8	16.3	<i>tenuicostatum</i>	Grey Shales Member
5	5.05	17.1	<i>tenuicostatum</i>	Grey Shales Member
3	4.75	16.1	<i>tenuicostatum</i>	Grey Shales Member
1	4.5	15.8	<i>tenuicostatum</i>	Grey Shales Member
43	2.3	16.4	<i>spinatum</i>	Cleveland Ironstone Formation
44	1.9	15.4	<i>Spinatum</i>	Cleveland Ironstone Formation
45	1.3	16.9	<i>Spinatum</i>	Cleveland Ironstone Formation

CALCULATING THE DURATION OF THE TIBETAN POSITIVE SULFUR ISOTOPE EXCURSION

In correlation A, the Tibetan excursion takes place in the Aalenian. A conservative upper estimate for its duration in this case would be the entire duration of the Aalenian which is estimated at 4 Myrs (2004). The magnitude of the excursion is 19.3‰, producing a minimum estimate of the rate of change of 4.8‰ Myr⁻¹. In correlation B the excursion in Tibet is correlated directly with the one in Yorkshire where it occurs within the lower portion of the *falciferum* zone. The biostratigraphy of the Yorkshire section is very detailed and the ages of Toarcian ammonite zonal boundaries have been estimated from intercalated radiometric dates (Cohen et al., 2004). From these dates, and the rate of change of the strontium isotope curve, the duration of the whole *falciferum* Zone has been estimated as 1.4 Myr (McArthur et al., 2000), serving as a conservative upper estimate for the duration of the Tibetan isotope excursion using correlation B. This produces a minimum rate of change of 13.7‰ Myr⁻¹.

APPLICATION OF THE KAH ET AL. (1994) SULFUR CYCLE MODEL TO THE EARLY JURASSIC

The model used by Kah et al. to estimate sulfate concentrations in the Proterozoic oceans uses modern weathering fluxes and an average isotopic enrichment of 35‰ for pyrite relative to the sulfate isotope composition, conditions acceptable as a starting point for an approximation of the Early Jurassic sulfur cycle. We have used their Figure 1 to estimate marine sulfate concentrations based on their maximum values of the relative pyrite burial flux of 0.6. This has the effect of maximising the estimated size of the sulfate reservoir to provide a conservative upper limit. The choice of the highest relative pyrite flux is also appropriate because of the enhanced pyrite burial associated with the depletion of oceanic oxygen levels. Weathering fluxes also increased during the OAE (2001), potentially balancing the elevated pyrite fluxes to a certain degree, although how significant this effect was is difficult to gauge.

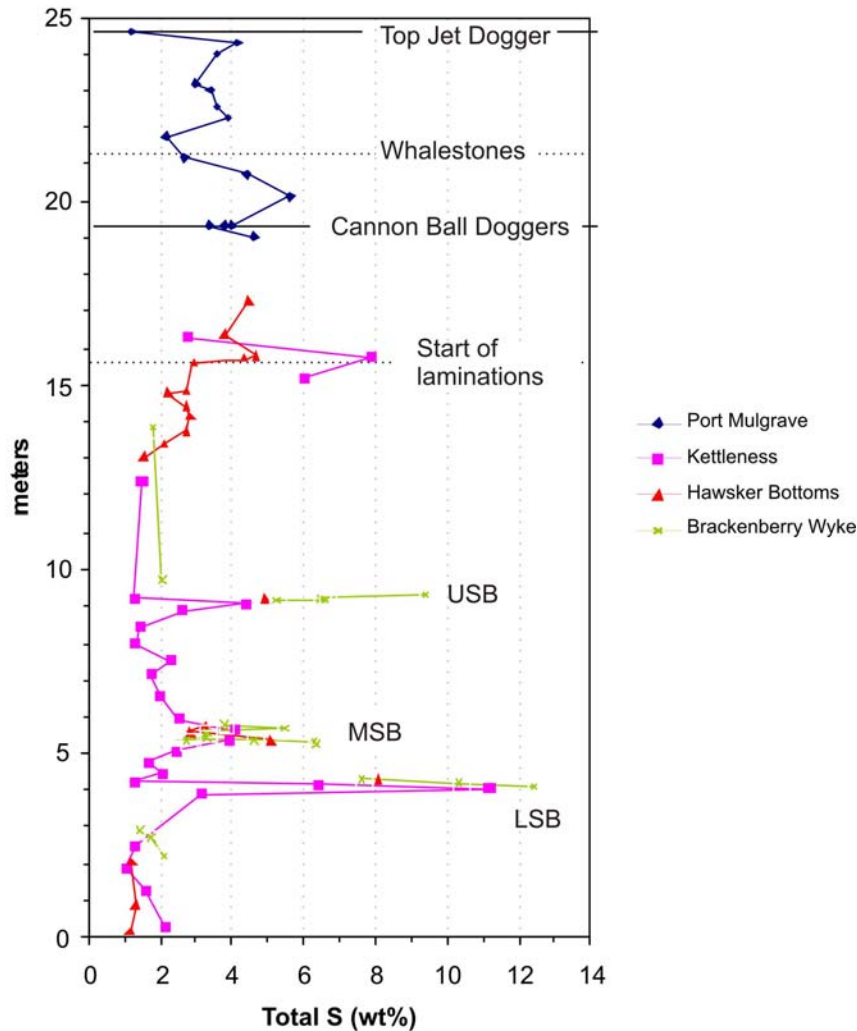


Figure DR5. Total S in the Grey Shales and Jet Rock of the north Yorkshire coast. Port Mulgrave data is from Dean, all other data is presented in Newton. LSB, MSB and USB refer to 'lower', 'middle' and 'upper sulfur band' respectively. Section heights are the same as those used for Yorkshire CAS data elsewhere in the paper.

References

- Cohen, A.S., Coe, A.L., Harding, S.M., and Schwark, L., 2004, Osmium isotope evidence for the regulation of atmospheric CO₂ by continental weathering: *Geology*, v. 32, p. 157-160.
- Dean, S.P., 1994, A Study of the Organic and Inorganic Geochemistry of Sulphur in Shales [PhD thesis]: Leeds, The University of Leeds.
- Jadoul, F., Berra, F., and Garzanti, E., 1998, The Tethys Himalayan passive margin from Late Triassic to Early Cretaceous (South Tibet): *Journal of Asian Earth Sciences*, v. 16, p. 173-194.
- Kah, L.C., Lyons, T.W., and Frank, T.D., 2004, Low marine sulphate and protracted oxygenation of the proterozoic biosphere: *Nature*, v. 431, p. 834-838.
- Newton, R.J., 2001, The Characterisation of Depositional Environments Using Fe, S and C Geochemistry [PhD thesis]: Leeds, The University of Leeds.
- Pálffy, J., Smith, P.L., and Mortensen, J.K., 2000, A U-Pb and Ar-40/Ar-39 time scale for the Jurassic: *Canadian Journal of Earth Sciences*, v. 37, p. 923-944.

- Utrilla, R., Pierre, C., Orti, F., and Pueyo, J.J., 1992, Oxygen and Sulfur Isotope Compositions As Indicators of the Origin of Mesozoic and Cenozoic Evaporites From Spain: *Chemical Geology*, v. 102, p. 229-244.
- Wignall, P.B., Hallam, A., Newton, R.J., Sha, J.G., Reeves, E., Mattioli, E., and Crowley, S., 2006, An eastern Tethyan (Tibetan) record of the Early Jurassic (Toarcian) mass extinction event: *Geobiology*, v. 4, p. 179-190.